ACCEPTED MANUSCRIPT
Review of Scientific Instruments
AIP Publishing
This is the author's peer reviewed, accepted manuscript. However, the online version of record will be different from this version once it has been copyedited and typeset.
PLEASE CITE THIS ARTICLE AS DOI: 10.1063/5.0267672

Design of an In-Vacuum Manipulator for Nuclear Diagnostics Development at the MIT Linear Electrostatic Ion Accelerator

M. Macon,[1] B. I. Buschmann,[1] M. Cufari,[1] S. G. Dannhoff,[1] A. DeVault,[1] T. E. Evans,[1] B. C. Foo,[1] T. M. Johnson,[1] J. H. Kunimune,[1] Y. Lawrence,[1] J. A. Pearcy,[1] B. L. Reichelt,[1] L. Russell,[1] N. Vanderloo,[1] J. Vargas,[1] C. W. Wink,[1] M. Gatu Johnson,[1] and J. A. Frenje[1]
Massachusetts Institute of Technology, Cambridge, Massachusetts, 02139

(Dated: 7 August 2025)

An ultra-high vacuum compatible manipulator known as the Diagnostic Manipulating Element (DiME) has been developed for the MIT Linear Electrostatic Ion Accelerator (LEIA) facility. The system was designed to reduce the resources dedicated towards the calibration process for Step-Range Filters (SRFs), CR-39 based proton spectrometers used in inertial confinement fusion (ICF) experiments at the Lawrence Livermore National Ignition facility (NIF) and the University of Rochester's OMEGA laser facility. To accurately account for variations in nominal filter thicknesses when analyzing experimental data, the spectrometers are calibrated at the MIT LEIA facility prior to use at other facilities. The system supports rapid prototyping and can reduce the time necessary for spectrometer calibration by 50%. The modular design of the DiME is described in this document to facilitate the implementation of similar design methods at other facilities focused on the development of nuclear fusion technologies.

I. INTRODUCTION

Nuclear diagnostics are used to evaluate the performance of inertial confinement fusion (ICF) implosions by measuring parameters such as areal density (ρR) and ion temperature (T_{ion}).[1–3] As such, nuclear diagnostics are vital for the operation of ongoing experiments conducted by various organizations at facilities like the National Ignition Facility (NIF) at Lawrence Livermore National Laboratory and the University of Rochester's OMEGA Laser Facility (OMEGA).[1,4–7] To reduce the costs and processing times associated with troubleshooting diagnostics while conducting an experiment, select diagnostics are calibrated at other facilities.[7] One such diagnostic is a CR-39-based proton spectrometer known as a Step-Range Filter (SRF), developed and calibrated at the MIT Linear Electrostatic Ion Accelerator Facility (LEIA).[5–7]

The SRF calibration process requires a significant allocation of LEIA facility resources.[6] Optimizing the calibration process allows more resources to be dedicated to other research projects at the LEIA facility. In pursuit of a system that improves the SRF calibration process while being adaptable to both pre-existing equipment and new research studies, an in-vacuum manipulator known as the "Diagnostic Manipulating Element" (DiME) has been implemented. The DiME allows novel diagnostic development techniques to be investigated without allocating a significant portion of facility resources.

Sec. II of this article describes the design objectives and constraints for the DiME system; Sec. III describes the design choices of the DiME; Sec. IV evaluates the system performance of the current DiME system and discusses future design considerations; Sec. V briefly concludes the discussion of the current system.

II. DESIGN OBJECTIVES AND CONSTRAINTS

A. Optimizing the Calibration of Proton Spectrometers

At the LEIA facility, the MIT High Energy Density Physics Group calibrates spectrometers used to measure the proton energy spectra emitted from DD and D^3He fusion reactions.[1,5–7] By measuring the proton energy spectra in different locations relative to the fusion implosion, the ρR asymmetries can be determined.[1,2]

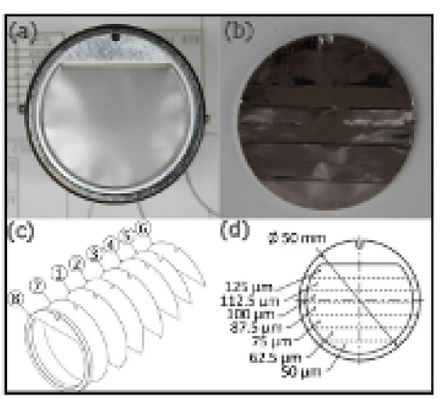

FIG. 1: A 7-section SRF, with diagrams detailing tantalum foil layer thicknesses. The four images show (a) the SRF as viewed from the target, (b) the SRF as viewed from the CR-39, (c) an exploded-view drawing of the assembly, and (d) the section thicknesses as viewed from the target. The SRF can be rotated to make sections horizontally or vertically adjacent. Reproduced with added text for clarity from Lahmann et al, Rev. Sci. Instrum. 92, 083506 (2021) with the permission of AIP Publishing.

SRF spectrometers reduce the energies of incoming protons using layers of tantalum foil arranged into sections (or "steps") of discrete thicknesses on an aluminum frame (See Fig. 1).[5,6] When passing through these sections, protons lose enough energy to be detectable by a CR-39 plastic plate, a

ACCEPTED MANUSCRIPT
Review of Scientific Instruments
AIP Publishing
This is the author's peer reviewed, accepted manuscript. However, the online version of record will be different from this version once it has been copyedited and typeset.
PLEASE CITE THIS ARTICLE AS DOI: 10.1063/5.0267672

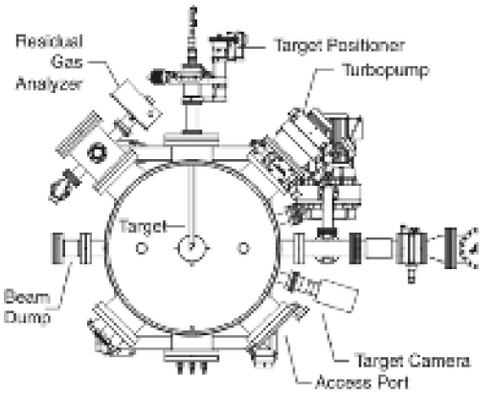

(a) Top-down sketch of target chamber. Reproduced from Sinenian et al, Rev. Sci. Instrum. 83, -53502 (2012) with the permission of AIP Publishing.

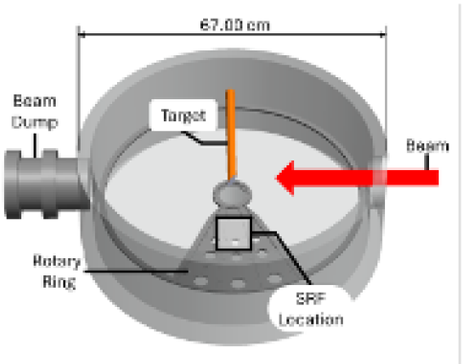

(b) Simplified CAD model of the target chamber with the rotary ring and ion beam (in red).

FIG. 2: Visualizations of the MIT LEIA target chamber. The target chamber is approximately 33 cm in radius and 25 cm tall.

nuclear track detector that can be processed after exposure to reaction products to determine the spectral information and yield of the reaction.[1,4–8]

To reduce the experimental uncertainty associated with nominal section thickness values, SRFs must be calibrated.[4,6] The LEIA can produce either 3-MeV DD-protons or 14.7-MeV D^3He-protons for the calibration process, depending on section thicknesses.[5,7] As fusion products pass through each section of filtering, their energies are recorded using a Surface Barrier Detector (SBD).[5–7] By varying the filter parameters within a theoretical model to match the collected data, the actual filter properties can be assessed and used in further analysis.[5–7] The number of sections that may be simultaneously calibrated depends on the size of the SBD and the cross-sectional area of each SRF section. To eliminate partial coverage of neighboring SRF sections by the SBD, an aperture is used to ensure the SBD is exposed to typically only one section.

To calibrate each SRF section, researchers were historically required to cycle the ultra-high vacuum (10^{-7} torr) and high voltage (150 kV) conditions of the LEIA, open the target chamber, and manually align the SRF-SBD configuration.[6,7] Repeatedly conducting this process for every SRF section is highly time-consuming. The primary objective of the DiME is to realign horizontally adjacent SRF sections with the SBD without cycling vacuum conditions, therefore substantially reducing the calibration time of an SRF.

B. Geometric and Environmental Constraints

Within the target chamber of the LEIA, the presence of ionized radiation, ultra-high vacuum conditions, and sensitive data collection instruments all enforced materials constraints on the DiME system. Materials that minimized outgassing and wear debris generation were required for the DiME to be compatible with these constraints.[8,9]

The LEIA accelerator produces DD and D^3He fusion products at rates up to 10^6 particles per second using an ErD_2 target that can be doped with ^3He.[7] To account for varying target depth when doped during the SRF calibration process, D^3He fusion product energies are measured using a separate 226Ra-calibrated SBD.[7] Instruments are placed on the rotary platform of the target chamber and aligned relative to the target (See Fig. 2). Due to the supporting structure of the rotary platform, instrument placement can induce angular deflection in the platform relative to the target, enforcing additional geometric and mass constraints on the DiME system.

III. DESIGN OVERVIEW

A. Mechanical Structure and Operation

The DiME was designed to allow researchers to realign horizontally adjacent sections of an SRF with the SBD aperture, without changing the distance to the target, using a slide mechanism constrained by an extension spring and actuated by a linear feedthrough attached to the target chamber. The slide allows for a custom SRF mount and auxiliary parts to be attached, and utilizes dry sliding bearings to reduce friction and wear debris generation (See Fig. 3).[9] Given the thread pitch of the target chamber's linear feedthrough, researchers can horizontally reposition the SRF with 0.01 millimeter resolution and lock the SRF in place.

To operate, researchers manually rotate the linear feedthrough dial until it reads that the slide has translated a specified distance. When the dial is rotated in the opposite direction, the extension spring provides enough force to move the slide back to the starting position.

B. Selected Materials

The environmental conditions generally associated with accelerators, in addition to project budget, guided the identification of materials suited for the DiME system. For most mechanical parts, uncoated 6061 series aluminum was used instead of stainless steel, due to its cost, weight, resistance to radiation-based activation, and machinability (See Fig. 4).[10]

ACCEPTED MANUSCRIPT
Review of Scientific Instruments
AIP Publishing
This is the author's peer reviewed, accepted manuscript. However, the online version of record will be different from this version once it has been copyedited and typeset.
PLEASE CITE THIS ARTICLE AS DOI: 10.1063/5.0267672

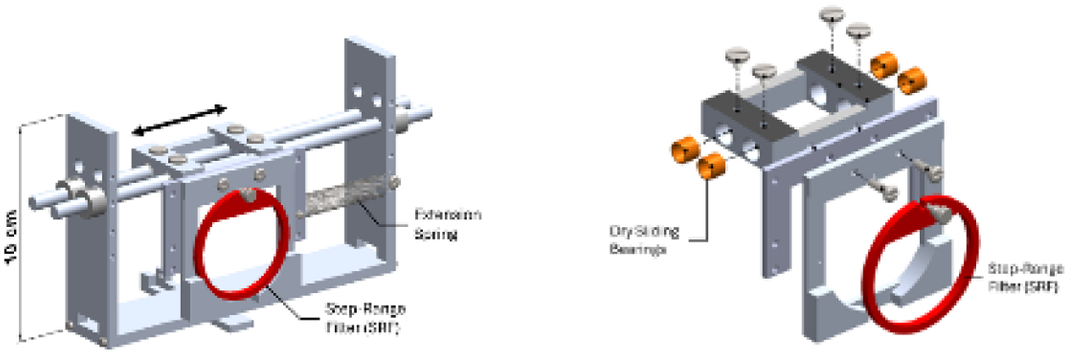

(a) Full assembly of the DiME. The black arrow represents the movement of the slide mechanism. SRF frame is indicated in red.

(b) Exploded view of the slide mechanism with diagnostic mount attached. PEEK/PTFE dry sliding bearings are indicated in orange.

FIG. 3: CAD Models of the DiME. The overall system dimensions are approximately 15 cm × 3 cm × 10 cm (l × w × h).

Aluminum with an anodized coating was avoided because of the increased level of outgassing derived from the surface coating.[10,11] All fasteners were made of austenitic stainless steels (300 series) due to their vacuum compatibility and commercial availability.[10] Galvanic corrosion occurring between aluminum components and stainless steel fasteners was mitigated by storing the system in a humidity-controlled chamber filled with nitrogen gas.

To reduce friction and wear, the slide mechanism features polished aluminum shafts and initially used PEEK bearings for dry lubrication, which were chosen for their low outgassing, radiation resilience, and wear resistance properties.[12–16] These bearings would be later exchanged for custom manufactured PTFE (Teflon) slide bearings, to further reduce friction in the system.[10] Understanding that PTFE becomes brittle under extended exposure to neutron and gamma radiation, the potential lifespan of these bearings will need to be evaluated based on additional processes besides SRF calibration that expose the system to such forms of radiation.[14,17] In addition, the cleaning procedures associated with the high wear debris generation of the PTFE bearings are currently being evaluated.[14]

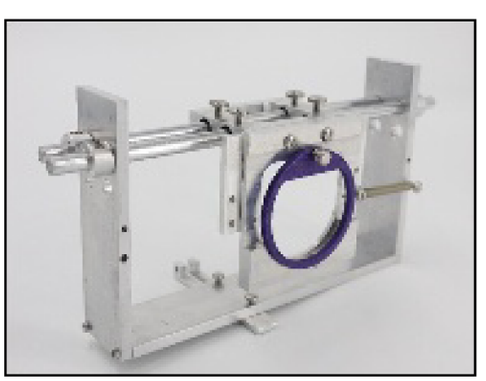

FIG. 4: Photo of the machined and fully assembled mechanical frame. A purple 3-D printed model of an SRF frame is placed for reference.

C. Design and Manufacturing Considerations

After numerous prototypes, it was found that a pulley-based actuation system that utilizes a spring was the most compatible with enforced design constraints, relative to actuation methods involving stepper motors, pneumatics, and a gear transmission system. However, cables and extension springs are known to undergo thermal deformation under particular conditions.[18] The extent to which these parts deform when exposed to the conditions of the LEIA target chamber is still being evaluated. Should parts permanently deform they can be easily and inexpensively replaced.

Given the specific geometric and material constraints enforced by the LEIA target chamber, components were manufactured by machining raw materials instead of purchasing commercially available subsystems and manipulation stages, with the exception of the linear feedthrough. The use of commercial subsystems would have required custom adapters for the unique geometry of the rotary platform and would have had to meet mass requirements to keep platform deflection within acceptable tolerance. To remove contaminants, parts were individually cleaned using ethanol prior to final assembly and use. By machining individual parts and designing the system to be assembled via screws, system upgrades, repairs, and geometric adjustments to the DiME can be installed relatively quickly, reducing research experiment downtime.

IV. RESULTS

A. System Performance

The DiME was placed into the LEIA target chamber for durability testing. With the DiME installed, ultra-high vacuum conditions were reached with no significant change to observed pump-down time, indicating that the materials of the system were vacuum compatible. Additionally, after exposing the DiME to the 125 keV-deuterium beam for approximately 6 hours, the DiME showed no obvious signs of material discoloration or deformation arising from ionizing radiation. This observed durability of the system affirms the findings of the

ACCEPTED MANUSCRIPT
Review of Scientific Instruments
AIP Publishing
This is the author's peer reviewed, accepted manuscript. However, the online version of record will be different from this version once it has been copyedited and typeset.
PLEASE CITE THIS ARTICLE AS DOI: 10.1063/5.0267672

prior literature discussed in the preceding sections.

The standard calibration process for an SRF requires 5 tasks to be completed for every filter section, with each section requiring a total of approximately 50 minutes to calibrate, as recorded by researchers in the MIT High Energy Density Physics Group (See Table I). The DiME system removes the need to cycle vacuum conditions in the LEIA target chamber and reduces the adjustment time of components to negligible amounts. By removing 3 tasks from the standard calibration process, the typical calibration rate for horizontally adjacent SRF sections was reduced by 50%, from approximately 50 minutes to 25 minutes per section.

The total percentage of time saved using the DiME depends on the SRF geometry, as modeled by Equation 1, where x is the total number of SRF sections, a is the number of vertically adjacent rows on the SRF, T_1 denotes the standard calibration rate per section, and T_2 denotes the calibration rate while using the DiME. Since the DiME features only horizontal movement, transitioning between vertically adjacent rows on an SRF requires the standard calibration process. This aspect of the system design is quantified by the constant a, and it depends on the orientation of the SRF as mounted on the DiME (in the case of Fig. 1, the 7 SRF sections shown can also be horizontally adjacent by rotating the frame 90 degrees). The total percentage time saved asymptotically approaches 50% (see Fig. 5) with an increasing number of sections.

TABLE I: Step-by-step calibration process for each section of filtering in an SRF, with and without using the DiME. Variables describing the total time per section are used in Eq. 1. These quantities are subject to minor fluctuations based on the researcher completing the tasks.

Process	Standard (min.)	With DiME (min.)
Vacuum Pump-Down	10	0
High Voltage	20	20
Accelerator Shot	5	5
Adjustment	5	0
Vacuum Pump-Up	5	0
Total (per Section)	$T_1 = 50$	$T_2 = 25$

$$\%TimeSaved = 100 - 100 \times \left(\frac{T_2 x + a(T_1 - T_2)}{T_1 x} \right) \quad (1)$$

A 3 X 3 sectioned SRF, with tantalum foil strips arranged such that there are only 5 sections that need calibration, was used as a reference to experimentally observe the time saved while using the DiME system. The calibration time for this SRF using the standard process was approximately 250 minutes, while the time recorded using the DiME was approximately 175 minutes, which represents an approximate 30% reduction in total calibration time (see Fig. 5).

B. Future Work

Potential upgrades to the DiME system include electronic remote controls used to mitigate the need to cycle high voltage conditions, and a mechanical redesign for vertical movement of mounted diagnostics. High voltage conditions prevent researchers from safely approaching the LEIA to operate

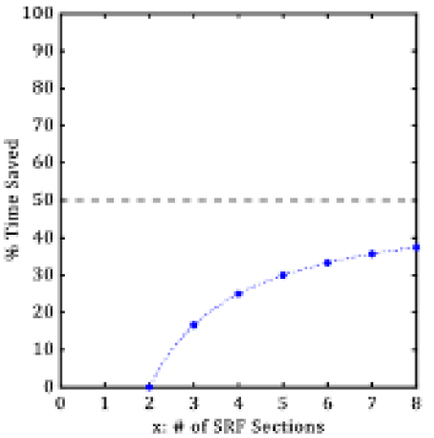

FIG. 5: Percentage of total time saved using the DiME for a 3 X 3 sectioned SRF. The horizontal dashed line represents the theoretical maximum time saved (50%). The curved line is included to emphasize the asymptotic nature of equation 1. The x-intercept represents the number of SRF sections subject to the standard calibration rate (one section for every vertically adjacent row). By using the DiME relative to the standard process, the percent time saved equaled approximately 30% for a 3 X 3 sectioned SRF.

the DiME, meaning that it must be cycled for every section change. Electronics would allow researchers to remotely control the system, preventing high voltage from being cycled. It is expected that remote controls would reduce the SRF calibration rate by a maximum additional 40% (See Table I), while the mechanical redesign would increase the versatility of the system by eliminating the need to use the standard calibration rate on vertically adjacent sections (See Equation 1). Additionally, remote controls could actively translate diagnostics during an experiment, allowing for new data collection techniques to be investigated.

V. CONCLUSIONS

The first iteration of the vacuum-compatible Diagnostic Manipulating Element (DiME) was successful in reducing the calibration rate of SRF diagnostics at the LEIA by 50%, through reducing the number of tasks required in the calibration process from 5 to 2. The successful operation of the system supports the findings of prior literature regarding the vacuum compatibility of materials and associated manufacturing processes. The modular design of the DiME allows the system to adapt to emerging technologies and diagnostic development processes at the LEIA facility. Similar design methods focusing on adaptability can be used at other facilities to further the development of other nuclear fusion diagnostics.

ACKNOWLEDGMENTS

The authors thank Rachel Shulman and Professor Mike Short for their guidance in academic writing, Dan Gilbert for their advice in manufacturing techniques, and Myles Stapel-

ACCEPTED MANUSCRIPT
Review of Scientific Instruments
AIP Publishing
This is the author's peer reviewed, accepted manuscript. However, the online version of record will be different from this version once it has been copyedited and typeset.
PLEASE CITE THIS ARTICLE AS DOI: 10.1063/5.0267672

berg and Simo Pajovic for their assistance in reviewing prior manuscript drafts. This project was funded through the MIT Undergraduate Research Opportunities Program and the MIT Fusion Undergraduate Scholars program, under the MIT Plasma Science and Fusion Center.

The work was also supported in part by the U.S. Department of Energy NNSA MIT Center-of-Excellence under Contract DE-NA0003868. This report was prepared as an account of work sponsored by an agency of the United States Government. Neither the United States Government nor any agency thereof, nor any of their employees, makes any warranty, express or implied, or assumes any legal liability or responsibility for the accuracy, completeness, or usefulness of any information, apparatus, product, or process disclosed, or represents that its use would not infringe privately owned rights. Reference herein to any specific commercial product, process, or service by trade name, trademark, manufacturer, or otherwise does not necessarily constitute or imply its endorsement, recommendation, or favoring by the United States Government or any agency thereof. The views and opinions of authors expressed herein do not necessarily state or reflect those of the United States Government or any agency thereof.

AUTHOR DECLARATIONS

A. Conflict of Interest

The Authors have no conflicts to disclose.

B. Author Contribution

M. Macon: Conceptualization (lead); Formal analysis (lead); Investigation (supporting); Methodology (equal); Project administration (equal); Resources (equal); Visualization (lead); Writing - original draft (lead); Writing - review and editing (equal). **B. I. Buschmann:** Conceptualization (supporting); Methodology (supporting); Resources (supporting); Writing - review and editing (supporting). **M. Cufari:** Conceptualization (supporting); Methodology (supporting); Resources (supporting). **S. G. Dannhoff:** Conceptualization (supporting); Methodology (supporting); Resources (supporting). **A. DeVault:** Conceptualization (supporting); Methodology (supporting); Resources (supporting); Writing - review and editing (supporting). **T. E. Evans:** Conceptualization (lead); Investigation (equal); Methodology (equal); Project administration (equal); Resources (equal); Supervision (lead); Writing - review and editing (equal). **B. C. Foo** Conceptualization (supporting); Methodology (supporting); Resources (supporting). **T. M. Johnson:** Investigation (lead); Methodology (supporting); Project administration (supporting); Software (supporting); Validation (lead). **J. H. Kunimune:** Conceptualization (supporting); Methodology (supporting); Resources (supporting); Writing - review and editing (supporting). **Y. Lawrence:** Conceptualization (supporting); Methodology (supporting); Resources (supporting). **J. A. Pearcy:** Conceptualization (supporting); Methodology (supporting); Resources (supporting). **B. L. Reichelt:** Conceptualization (supporting); Methodology (supporting); Resources (supporting); Writing - review and editing (supporting). **L. Russel:** Investigation (equal); Validation (supporting). **N. Vanderloo:** Conceptualization (supporting); Methodology (supporting); Resources (supporting). **J. Vargas:** Conceptualization (supporting); Resources (supporting); Methodology (supporting); Writing - review and editing (supporting). **C. W. Wink:** Conceptualization (supporting); Methodology (supporting); Resources (supporting); Writing - review and editing (supporting). **M. Gatu Johnson:** Supervision (supporting); Writing - review and editing (supporting). **J. A. Frenje:** Supervision (supporting); Writing - review and editing (supporting).

DATA AVAILABILITY STATEMENT

Data sharing is not applicable to this article as no new data were created or analyzed in this study.

REFERENCES

No generative AI was used in this work.

[1]M. G. Johnson, Review of Scientific Instruments **94**, 021104 (2023).
[2]C. K. Li, D. G. Hicks, F. H. Séguin, J. A. Frenje, R. D. Petrasso, J. M. Soures, P. B. Radha, V. Y. Glebov, C. Stoeckl, D. R. Harding, J. P. Knauer, R. Kremens, F. J. Marshall, D. D. Meyerhofer, S. Skupsky, S. Roberts, C. Sorce, T. C. Sangster, T. W. Phillips, M. D. Cable, and R. J. Leeper, Physics of Plasmas **7**, 2578 (2000).
[3]F. H. Séguin, C. K. Li, J. A. Frenje, D. G. Hicks, K. M. Green, S. Kurebayashi, R. D. Petrasso, J. M. Soures, D. D. Meyerhofer, V. Y. Glebov, P. B. Radha, C. Stoeckl, S. Roberts, C. Sorce, T. C. Sangster, M. D. Cable, K. Fletcher, and S. Padalino, Physics of Plasmas **9**, 2725 (2002).
[4]F. H. Séguin, J. A. Frenje, C. K. Li, D. G. Hicks, S. Kurebayashi, J. R. Rygg, B.-E. Schwartz, R. D. Petrasso, S. Roberts, J. M. Soures, D. D. Meyerhofer, T. C. Sangster, J. P. Knauer, C. Sorce, V. Y. Glebov, C. Stoeckl, T. W. Phillips, R. J. Leeper, K. Fletcher, and S. Padalino, Review of Scientific Instruments **74**, 975 (2003).
[5]M. J. Rosenberg, A. B. Zylstra, J. A. Frenje, H. G. Rinderknecht, M. G. Johnson, C. J. Waugh, F. H. Séguin, H. Sio, N. Sinenian, C. K. Li, R. D. Petrasso, V. Y. Glebov, M. Hohenberger, C. Stoeckl, T. C. Sangster, C. B. Yeamans, S. LePape, A. J. Mackinnon, R. M. Bionta, B. Talison, D. T. Casey, O. L. Landen, M. J. Moran, R. A. Zacharias, J. D. Kilkenny, and A. Nikroo, Review of Scientific Instruments **85**, 103504 (2014).
[6]B. Lahmann, M. Johnson, J. Frenje, A. Birkel, P. Adrian, N. Kabadi, J. Kunimune, T. Johnson, J. Pearcy, B. Reichelt, F. Séguin, G. Sutcliffe, and R. Petrasso, Review of Scientific Instruments **92**, 083506 (2021).
[7]N. Sinenian, M. J.-E. Manuel, A. B. Zylstra, M. Rosenberg, C. J. Waugh, H. G. Rinderknecht, D. T. Casey, H. Sio, J. K. Ruszczynski, L. Zhou, M. G. Johnson, J. A. Frenje, F. H. Séguin, C. K. Li, R. D. Petrasso, C. L. Ruiz, and R. J. Leeper, Review of Scientific Instruments **83**, 043502 (2012).
[8]B. Lahmann, M. G. Johnson, J. A. Frenje, Y. Y. Glebov, H. G. Rinderknecht, F. H. Séguin, G. Sutcliffe, and R. D. Petrasso, Review of Scientific Instruments **91**, 053502 (2020).
[9]L. Lilje, "Controlling Particulates and Dust in Vacuum Systems," Course Proceedings (CERN Accelerator School, 2017).
[10]Y. Li and X. Liu, "Vacuum Science and Technology for Accelerator Vacuum Systems," (2017).
[11]Y. Luo, X. Wu, K. Wang, and Y. Wang, Applied Surface Science **502**, 144166 (2020).
[12]M. Tavlet and H. van der Burgt, "Radiation resistance and other safety aspects of high-performance plastics by ERTA," (1994).
[13]K. Elleuch, S. Mezlini, S. Fouvry, and P. Kapsa, Industrial Lubrication and Tribology **55**, 279 (2003).
[14]S. Qu, J. Penaranda, and S.-S. Wang (2016).
[15]S. Panda, M. Sarangi, and S. K. R. Chowdhury, Polymer Testing **77**, 105880 (2019).
[16]J. Chen, Q. Guo, S. Zhang, X. Wang, and X. Shao, Procedia Engineering IUMRS International Conference in Asia 2011, **36**, 285 (2012).
[17]O. K. Harling, G. E. Kohse, and K. J. Riley, Journal of Nuclear Materials **304**, 83 (2002).

[18]B. T. Werner, B. R. Antoun, and G. B. Sartor, "Thermal Degradation of Extension Springs." Tech. Rep. SAND2015-1555C (Sandia National Lab. (SNL-CA), Livermore, CA (United States), 2015).

AIP Publishing
Review of Scientific Instruments
ACCEPTED MANUSCRIPT
This is the author's peer reviewed, accepted manuscript. However, the online version of record will be different from this version once it has been copyedited and typeset.
PLEASE CITE THIS ARTICLE AS DOI: 10.1063/5.0267672